Coseismic and Postseismic Displacement of 2011 Mw 6.8 Tarlay Earthquake, Myanmar using InSAR Techniques and Inversion Analysis

Pattama Phodee, Itthi Trisirisatayawong and Anuphao Aobpaet

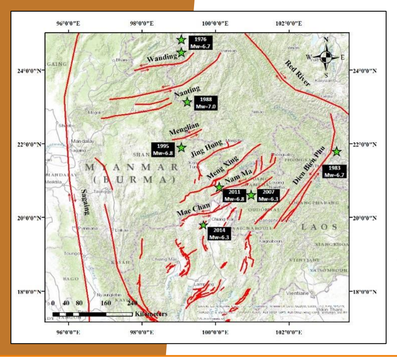

Fig. 1. Map of faults in Shan fault system. Green stars represent epicenters of large earthquake (M_w>6.3) events since 1976. The faults are members of a group of left-lateral faults in Shan fault system posing as network triangle faults between Sagaing fault in Myanmar and Red River fault in northern Vietnam. Many large earthquakes occurred in this fault system since late 20th century.

Fig. 1.Map of faults in Shan fault system. Green stars represent epicenters of large earthquake (Mw>6.3) events since 1976.

InSAR for Coseismic deformation detection.

In the previous study, 4 ALOS PALSAR Single Look Complex images in both ascending track 126 and descending track 486 orbits were acquired before and after earthquake. This is shown in the Table 1 below.

Table 1. Acquisition details of ALOS PALSAR data (fine beam mode with HH- polarization).

Path	Master date	Slave date	Perpendicular Baseline (meter)	Temporal Baseline (day)
Ascending	16 February 2011	3 April 2011	48.7	46
Descending	14 February 2011	1 April 2011	436.2	46

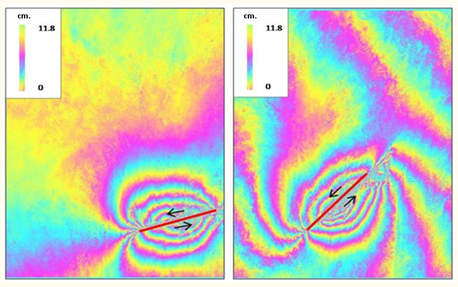

Fig. 2.Differntial interferograms formation using 2-pass InSAR from ascending (left) and descending path (right), 1 color cycles=11.8 centimeters and red line is Nam Ma fault.

Fig. 2 the results reveal displacement in line-of-sight direction (LOS). From the interferogram, a 1.2 meters left-lateral offset in the radar LOS can be estimated across the fault. Small offsets around 12 centimeters are observable at distance of more than 20 kilometers from the epicenter. The observed coseismic motions suggest that earthquake could also have impact on Mae Chan fault, around 50 kilometers to the south of the earthquake.

Inversion for fault geometry parameters by Single-patch model.

Figure 3 shows the coseismic displacement from downsampled interferogram. We found the difference in residuals in the descending (± 0.2 meters.) path which is larger than ascending path. It is important to note that the ascending path shows entirely satisfied results while the descending path contrary performance presents noticeably large residuals in particular parts which however do not have huge impact to the whole process.

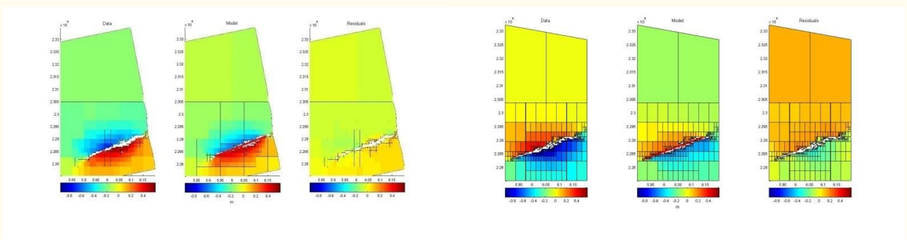

Fig. 3.Coseismic displacement in LOS direction of the ascending (left) and descending (right) path from downsampled interferogram, model and residual respectively. We found that the slip from both model are maximum varied 0.27 meters. The 2.5 meters slip value from Single-patch model is used in coulomb stress change for slip distribution

Figure 4 The maximum slip is 2.77 meters in the depth 5-6 kilometers. The major group of slip rate locates between 3-8 kilometers depth in the middle and west of Nam Ma fault. The maximum number of slip near the surface is 1.95 meters (< 1 kilometer at deep) and less than the number of slip rate at 3-8 kilometers below surface.

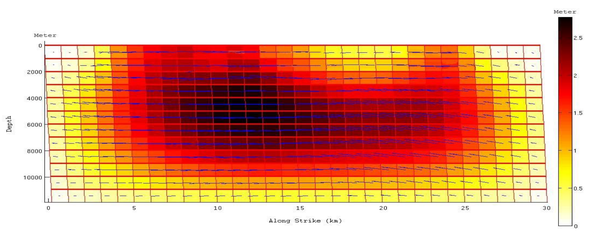

Fig. 4.Distribution of fault slip in Tarlay earthquake, maximum slip is 2.77 meters at depth 5-6 kilometers. Most of occurring is approximately 10 kilometers below surface.

Comparison of slip distribution with field data

Figure 5 reveals a field survey data after Tarlay earthquake Myint, et al., the yellow points in the image indicate the position of field survey in the areas. The yellow numbers in the image indicate the offset values in the areas. The total length of fault is approximately 30 kilometers and the maximum offset value is 1.25 meters in the western of the fault. The graph below displayed a comparison between the slip obtained from field survey and the slip distribution using Multi-patch model. The comparison between those data is estimated base on coordinate information , so the starting point from field survey will begin at kilometer 10.

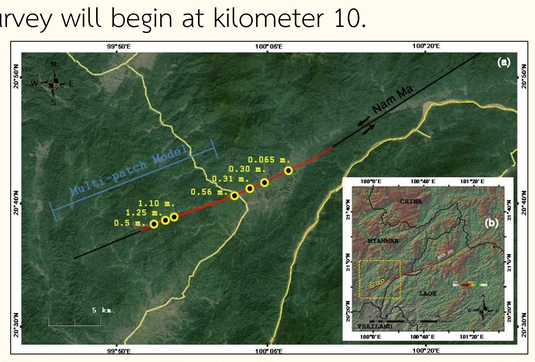

Fig. 5.Map shows the position of the field survey data on the west side of the Nam Ma fault. The blue line indicates the length of fault which is resulted from Multi-patch model analysis. The origins used in comparison between model analysis and field survey analysis are unequal.

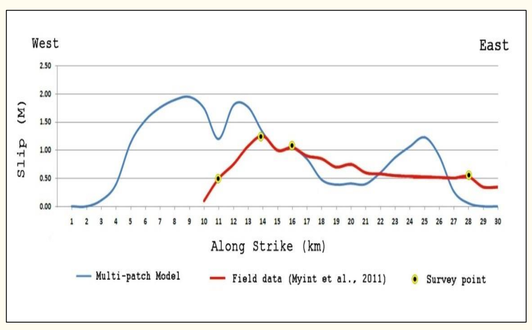

Fig. 6.The graph shows a comparison of the slip distribution. Red line is obtained from the field survey, yellow points indicate field survey locations , and the blue line is slip distribution of the results.

Coulomb stress change computation

Fig. 7 Nam Ma fault releases its stress during the earthquake, and the stress is re-distributed to surrounding area, especially near the Mae Chan fault slips. If we primarily consider Mae Chan fault, the east end and of Mae Chan fault could be failure caused by the increasingly of the stress as indicated in the maximum value of coulomb stress scale around 0.6 bar. At the same time, the west and middle of the fault are stress shadow zone.

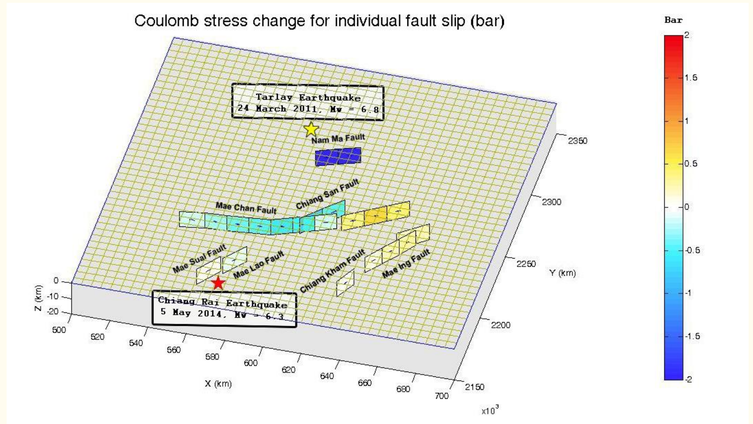

Fig. 7.Coulomb stress change result on Mae Chan and nearby fault in upper northern of Thailand after the Tarlay earthquake. Red star shows the epicenter of M_w=6.3 Chiang Rai earthquake, occurring on 5 May 2014.

Time-series InSAR for postseismic deformation detection.

The postseismic investigation is performed by processing the 19 Radarsat-2 images (Beam type: F3N, Incidence angle: 42°) with Time-series InSAR analysis. The result from PS technique reveals the postseismic deformation of Tarlay earthquake spanning approximately two years. There are more than 147,000 PS points of ascending path with LOS displacement rate between -24.4 to 34.5 millimeters per year.

The results show the positive range change (blue) i.e. moving away from the sensor in the southern part of Nam Ma fault while the northern show negative range change (red) meaning moving toward the sensor direction. The result was consistent with left-lateral fault movement. The white dash line shows an imaginary transect across the Nam Ma fault line. Figure 8(b) shows profile of this transect. It can be seen that the LOS velocities are symmetrical across the fault. The displacement pattern is consistent with Reid's elastic rebound model in postseismic phase.

8a 8b

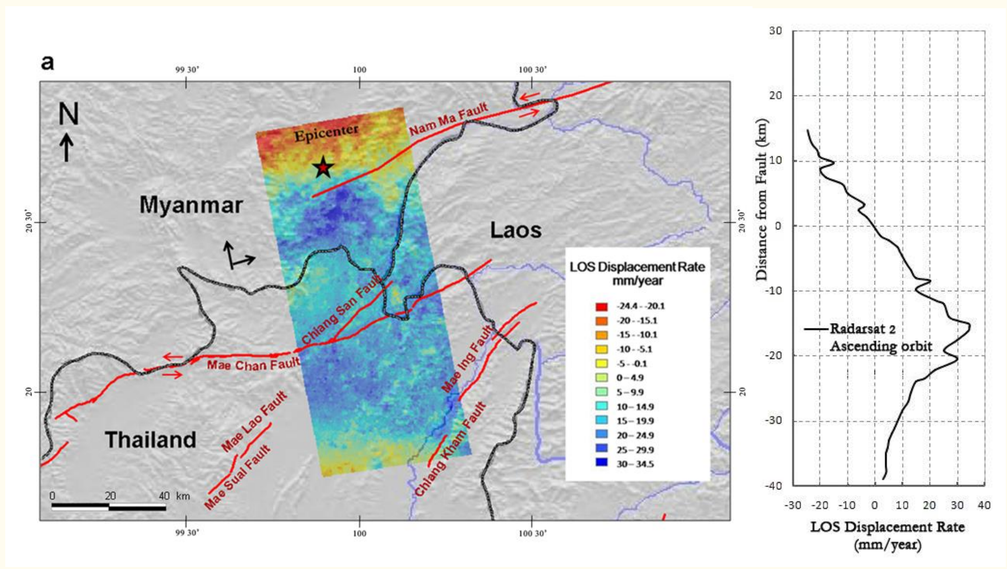

Fig. 8(a).Displacement rate (milimeter/year) in Nam Ma and Mae Chan fault region from Time-series InSAR analysis of a suite of 19 Radarsat-2 imageries from June 2011 to May 2013. Dark arrows show direction of Radarsat-2 trajectory and its LOS. Negative range changes (red) were detected in the area north of Nam Ma fault and positive range change (blue) in the south of the fault. White dash line shows an imaginary transect crossing Nam Ma fault line. b) The profile of the transect shown in a).

Conclusion

In this study, we investigate the March 24th, 2011 M_w=6.8 Tarlay earthquake, Myanmar using InSAR and inversion analysis. We firstly invert InSAR coseismic displacement from our previous study. The inversions for fault parameters are carried out in both Single and Multi-patch model. The coseismic slip of 2.5 meters from Single-patch solution is then combined with long-term slip rate from geomorphological study, resulting in an estimate of 1,040-4,160 years recurrence period. Then, coulomb stress changes on nearby faults in northern Thailand are calculated. It is found that stress in western and middle segments of Mae Chan fault decreases significantly while stress increase in eastern segment of Mae Chan, Mae Ing and Chiang Kham fault. Finally, the results from PSInSAR of 29 Radarsat-2 images reveal postseismic displacement rates between -24.4 to 34.5 millimeters per year.

REFERENCES:

[1] J. McCaughey and P. Tapponnier, (2011). *Myanmar earthquake of March 24, 2011 - Magnitude 6.8* [Online]. Available: http://www.earthobservatory.sg/media/news-and-features/295-myanmar-earthquake-of-march-24th-magnitude-68.html

[2] I. Trisirisatayawong, A. Hooper and A. Aobpaet, "Co-seismic Displacement of 24-March 2011 M_w 6.8 Mong Hpayak Earthquake, Myanmar," in *FRINGE Workshop ESA.*, Frascati, Italy, 2011.

[3] R. Lacassin, A. Replumaz and P.H. Leloup, "Hairpin river loop and slip sense inversion on SE-Asian strike-slip faults," *Geology*, vol. 26, no. 8, pp. 703-706, August, 1998.

[4] T.J. Wright, "Remote monitoring of the earthquake cycle using satellite radar interferometry," *Philosophical Transactions of the Royal Society of London*, vol. 360, no. 1801, pp. 2873-2888, December, 2002.

[5] Y. Okada, "Surface deformation due to shear and tensile faults in a half space," *Bulletin of the Seismological Society of America*, vol. 75, no. 4, pp. 1135–1154, August, 1985.

[6] A. Hooper, "Inversion of InSAR data for the estimation of movement on faults," in *GEO2TECDI-SONG InSAR Workshop*, Bangkok, Thailand, 2011.

[7] S. Toda, R.S. Stein, V. Sevilgen and J. Lin, (2011). *Coulomb 3.3 graphic-rich deformation and stress-change software for earthquake, tectonic, and volcano research and teaching user guide* [Online]. Available: http://usgsprojects.org/coulomb/Coulomb33of2011-1060.pdf.

[8] A. Hooper, P. Segall and H. Zebker, "Persistent scatterer interferometric synthetic aperture radar for crustal deformation analysis, with application to Volcáno Alcedo, Galapagos," *Journal of Geophysical Research*, vol. 112, no.B07407, pp. 1-21, July, 2007.

[9] U.T. Myint, U.S.T. Tun, U.S. NgweKhine, U.S. Htwezaw, M. Thant, Y.M.M. Htwe, *"Myanmar Earthquake Committee Tarlay Earthquake (6.8 Magnitude, 24 March 2011),"* Survey trip Pre-report.